Research Paper
Computational Methods for Differential Equations
http://cmde.tabrizu.ac.ir
Vol. 12, No. 1, 2024, pp. 117-135
DOI:10.22034/cmde.2023.53596.2256

A one-step algorithm for strongly non-linear full fractional duffing equations

Jafar Biazar* **and Hamed Ebrahimi**
Department of Applied Mathematics, Faculty of Mathematical Sciences, University of Guilan, P.O. Box 41335-1914, P.C.4193822697, Rasht, Iran.

Abstract

In the current study, a one-step numerical algorithm is presented to solve strongly non-linear full fractional duffing equations. A new fractional-order operational matrix of integration via quasi-hat functions (QHFs) is introduced. Utilizing the operational matrices of QHFs, the main problem will be transformed into a number of univariate polynomial equations. Absolute errors of the results in approximations and convergence analysis are addressed. Ultimately, five examples are provided to illustrate the capabilities of this algorithm. The numerical results are illustrated in some Tables and Figures, for different values of the parameters α *and* β.

Keywords. Fractional Duffing differential equations, Numerical algorithms, Strongly nonlinear, Quasi-hat function, Fractional operational matrix.
2010 Mathematics Subject Classification. 26A33, 65D15, 46Txx, 33Exx.

1. Introduction

The mathematical modeling of many phenomena in various branches of science leads to non-linear differential equations. A differential equation handles the damped, driven oscillator [1].
Many scientists have applied fractional calculus to describe their models in sciences and engineering fields [19]. One of the most popular differential equations are the Duffing-type oscillator, which was first introduced by Georg Duffing in 1918 [17]. A physical system that consists of a steel ball of mass m , two strong magnets, and a light flexible rod. Figure 1 shows a Duffing oscillator system. These kinds of equations appear in the field of signal processing [31], foundations and bridges [9], waves, and brain modelling [4, 13], etc. In most cases, it is impossible to obtain an analytical solution to differential equations. As a result, the introduction of numerical algorithms is very important to obtain approximate solutions, so various numerical methods were developed to solve these types of equations by many researchers. Some of the prominent methods are Adomian decomposition, Homotopy analysis [8, 12], modified differential transform [21, 24], collocation [7, 23], Galerkin [3, 6], product integration [5, 28], Rationalized haar wavelets [10, 15], Jacobi wavelets [18], Chebyshev wavelets [2], Hermite cubic splines [11], Taylor series [14], etc.
(1): If a system is modeled by fractional order, a higher-order system can be modeled by a lower-order model.
(2): The nature of many systems makes it possible to model them more accurately using fractional functional equations.
(3): In general, a fractional model includes an integer-order model, as well.
In this work, we consider the following non-linear full fractional duffing equation:

$$\begin{aligned} &{}_0^C D_t^{\beta} u(t) + \mu_0 {}_0^C D_t^{\alpha} u(t) = g(t) + \sum_{k=1}^{4} \mu_k \big(u^{2k-1}(t)\big),\ 1 < \beta \leq 2,\ 0 < \alpha \leq 1, \\ &u^{(i)}(0) = u_0^{(i)},\ \ i = 0, 1, ..., \lceil \beta \rceil - 1,\ t \in I(T), \end{aligned} \tag{1.1}$$

where $u(t)$ is an unknown function to be determined, $\mu_k,\ k = 0, ..., 4$ are the appropriate parameters, $g(t)$ is a known continuous function on $I(T) := [0, T]$, and ${}_0^C D_t^{\beta}$ is the Caputo fractional differential operator of order β. Some numerical methods convert such a Duffing equation into a system of algebraic equations that can be easily solved. Yusufoglu has proposed the Laplace decomposition algorithm to solve a Duffing equation [33]. Rad et al. applied a numerical

Received: 27 September 2022 ; Accepted: 17 May 2023.
$*$ Corresponding author. Email: biazar@guilan.ac.ir.

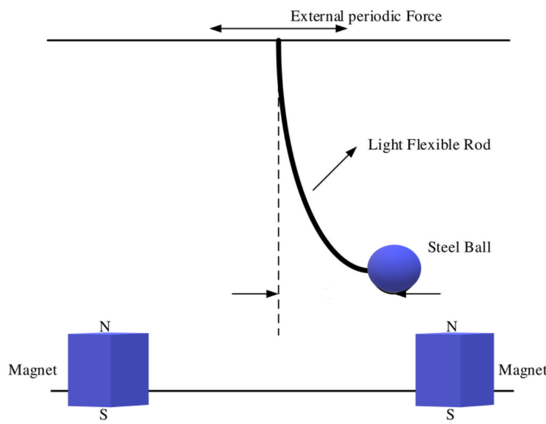

FIGURE 1. Duffing oscillator system.

method based on the radial basis functions for solving the nonlinearly controlled Duffing oscillator [27]. Pirmohabbati et al. used block-pulse wavelets to solve non-linear oscillatory and vibration equations [25]. Zhang et al. applied a finite difference scheme to give approximate solutions for a class of the fractional Duffing equations [34]. Issa et al. utilized the shifted Gegenbauer polynomial to solve a one-dimensional space fractional diffusion equation [16]. Also, a numerical solution to a non-linear Duffing equation via a hybrid method is suggested by Torkzadeh [29].
In this paper, we introduce a numerical algorithm for the problem (1.1) in terms of QHFs. The present work discusses some of the properties of Riemann-Liouville integral operators to solve the non-linear full fractional Duffing equations. Using the operational matrix method, the principal problem will be reduced to solving several non-linear univariate polynomial equations. In section 2, some basic definitions and characteristics of the fractional calculus are presented. Section 3 is devoted to introducing the operational matrix of QHFs basis. Fourth section studies the absolute error of approximation of a function by a truncated series of QHFs. The fifth section presents a numerical method for the problem (1.1).
The convergence analysis of the proposed method is discussed in section 6. To demonstrate the validity and accuracy of the utilized approach, five numerical examples are provided in section 7, and the paper ends in section 8, with a conclusion and discussion.

2. Basic concepts and definitions

In this section, some definitions, properties, and preliminaries of the fractional calculus theory that will be used in this manuscript are explained.

2.1. **Fractional order integral and differential operators.**

Definition 2.1. Let $n-1 <\alpha \leq n$, $\alpha > 0$, $t > 0$. The operator ${}_0^cD_t^\alpha u(t)$ defined as [26]

$$ {}_0^cD_t^\alpha u(t) = \begin{cases} \frac{1}{\Gamma(n-\alpha)} \int_0^t (t-\tau)^{n-\alpha-1} \frac{d^n}{d\tau^n} u(\tau) d\tau, & n-1 < \alpha \leq n, \\ u^{(n)}(t), & \alpha = n\,, \end{cases} \tag{2.1} $$

is called the Caputo fractional differential operator of order α.

Definition 2.2. The Riemann-Liouville integral operator of order α is defined as [26]

$$I_t^{\alpha}u(t) = \frac{1}{\Gamma(\alpha)}\int_0^t (t-\tau)^{\alpha-1}u(\tau)d\tau, \tag{2.2}$$

where $\Gamma(x)$ is the gamma function: $\Gamma(x) = \int_0^{\infty} t^{x-1}e^{-t}dt$.

The Riemann–Liouville integral operator and the Caputo fractional derivative operator (2.1) satisfies the following properties [26]:

$$I_t^{\alpha}({}_{\circ}^{C}D_t^{\alpha}u(t)) = u(t) - \sum_{i=0}^{n-1} u^{(i)}(0)\frac{t^i}{i!}, \qquad n-1<\alpha\leq n, \tag{2.3}$$

and we get

$$I_t^{\beta}({}_{\circ}^{C}D_t^{\alpha}u(t)) = \left(I_t^{\beta-\alpha}u(t)\right) - \left(\sum_{i=0}^{n-1}\frac{u^{(i)}(0)}{i!}I_t^{\beta-\alpha}t^i\right),\ n-1<\alpha\leq n,\ \alpha<\beta. \tag{2.4}$$

2.2. **Definition of QHFs.** Let us state here some definitions and properties regarding QHFs. These functions are established based on the idea of the hat functions [7, 30]. Quasi-hat functions are defined on the closed interval $[0,T]$, and has a hat-like shape, the interval is divided into n subintervals $[ih,(i+1)h]$, $i=0,1,2,...,n-1$, of equal lengths h, where $h=\frac{T}{n}$, and $n\geq 2$ is an even positive integer.
QHFs are defined as follows for i even, and $0\leq i\leq n$;

$$\phi_i(t) = \begin{cases} \frac{1}{2h^2}(t-(i+1)h)(t-(i+2)h), & ih\leq t<(i+2)h, \\ 0, & otherwise, \end{cases} \tag{2.5}$$

when i is odd, and $1\leq i\leq n-1$;

$$\phi_i(t) = \begin{cases} -\frac{1}{2h^2}(t-(i-1)h)(t-(i+2)h), & (i-1)h\leq t<(i+1)h, \\ 0, & otherwise. \end{cases} \tag{2.6}$$

A function $u(t)$ can be expressed in terms of QHFs as follows

$$u(t) \simeq u_n(t) = \sum_{i=0}^{n} a_i\phi_i(t) = \mathrm{A}^{\mathrm{T}}\Phi(t) = \Phi(t)^{\mathrm{T}}\mathrm{A}, \tag{2.7}$$

so that

$$\Phi(t) = [\phi_0(t),\phi_1(t),...,\phi_n(t)]^T, \tag{2.8}$$

and

$$\mathrm{A} = [a_0,a_1,...,a_n]^T. \tag{2.9}$$

wherein $a_i = u(ih)$, $i=0,...,n$, are unknown coefficients of the QHFs.

2.2.1. *Properties of QHFs.* The following properties can be achieved by using the QHFs definition

$$\sum_{i=0}^{n}\phi_i(t) = 1, \qquad \phi_i(jh) = \begin{cases} 1, & i=j, \\ 0, & i\neq j. \end{cases} \tag{2.10}$$

Multiplying both sides of this summation to $\phi_j(t)$, gives

$$\left(\sum_{i=0}^{n}\phi_j(t)\phi_i(t)\right) = \phi_j(t), \tag{2.11}$$

thus, for $t = jh$, we attain

$$\begin{aligned}
&\sum_{i=0}^{n} \phi_j(jh)\phi_i(jh) = \phi_j(jh), \\
&[(\phi_j(jh)\phi_0(jh)) + ... + (\phi_j(jh)\phi_j(jh)) + ... + (\phi_j(jh)\phi_n(jh))] = \psi_j(jh), \\
&[(\phi_j(jh) \times 0) + ... + (\phi_j(jh) \times \phi_j(jh)) + ... + (\phi_j(jh) \times 0)] = \phi_j(jh),
\end{aligned} \tag{2.12}$$

consequently

$$\phi_j(jh)\phi_j(jh) = \phi_j(jh). \tag{2.13}$$

Taking these properties, one has

$$\phi_i(t)\phi_j(t) \approx \begin{cases} \phi_i(t), & j = i, \\ 0, & j \neq i. \end{cases} \tag{2.14}$$

Then, from the relations (2.14) and (2.8), it can be concluded that

$$\Phi(t)\Phi^T(t) \simeq diag[\phi_0(t),\, \phi_1(t), ...,\, \phi_{n-1}(t),\, \phi_n(t)]^T. \tag{2.15}$$

2.2.2. *Non-linear approximation of QHFs.* Using (2.15) and (2.7), $u^m(t)$, $m = 1, 2, ...,$ can be calculated as follows

$$\begin{aligned}
u^2(\mathrm{t}) \simeq& \mathrm{A}^T\Phi(t)\Phi^T(t)\mathrm{A} = \mathrm{A}^T diag(\Phi(t))A = \mathrm{A}^T diag(A)\Phi(t) \\
&= \mathrm{A}_2^T\Phi(t), \quad \mathrm{A}_2 = [a_0^2, a_1^2, ..., a_n^2]^T, \\
u^3(\mathrm{t}) \simeq& u^2(\mathrm{t})u(\mathrm{t}) = \mathrm{A}_2^T\Phi(t)\Phi^T(t)\mathrm{A} = \mathrm{A}_2^T diag(\Phi(t))A = \mathrm{A}_2^T diag(A)\Phi(t) \\
&= \mathrm{A}_3^T\Phi(t), \quad \mathrm{A}_3 = [a_0^3, a_1^3, ..., a_n^3]^T, \\
&\vdots \\
u^m(t) \simeq& \sum_{i=0}^{n} {a_i}^m\phi_i(t) = \mathrm{A}_m^T\Phi(t), \quad \mathrm{A}_m = [a_0^m, a_1^m, ..., a_n^m]^T.
\end{aligned} \tag{2.16}$$

3. Operational matrices of QHFs

In this part of the study, we obtain the fractional-order integral operational matrix using quasi-hat functions.

3.1. **Fractional order operational matrix of integration.** We state the following theorem:

Theorem 3.1. *Let $\Phi(t)$ be given by (2.8) and $\alpha > 0$, then*

$$I_t^\alpha\Phi(t) \simeq Q^\alpha\Phi(t). \tag{3.1}$$

where Q^α is called $(n+1)\times(n+1)$ operational matrix of fractional integration of order α and is defined as follows:

$$Q^{(\alpha)} = \frac{h^\alpha}{2\Gamma(\alpha+3)} \begin{pmatrix}
0 & \rho_1 & \rho_2 & \rho_3 & \rho_4 & \cdots & \rho_{n-1} & \rho_n \\
0 & \sigma_1 & \sigma_2 & \sigma_3 & \sigma_4 & \cdots & \sigma_{n-1} & \sigma_n \\
0 & 0 & 0 & \rho_1 & \rho_2 & \cdots & \rho_{n-3} & \rho_{n-2} \\
0 & 0 & 0 & \sigma_1 & \sigma_2 & \cdots & \sigma_{n-3} & \sigma_{n-2} \\
0 & 0 & 0 & 0 & 0 & \cdots & \vdots & \vdots \\
\vdots & \vdots & \vdots & \vdots & \vdots & & \vdots & \vdots \\
0 & 0 & 0 & 0 & 0 & \cdots & \rho_1 & \rho_2 \\
0 & 0 & 0 & 0 & 0 & & \sigma_1 & \sigma_2 \\
0 & 0 & 0 & 0 & 0 & \cdots & 0 & 0
\end{pmatrix}, \tag{3.2}$$

where

$$\begin{aligned}
&\rho_1 = \alpha\left(2\alpha+3\right),\\
&\rho_k = \Big(k^{\alpha+1}(2k-3\alpha-6) + 2k^{\alpha}(\alpha+1)(\alpha+2) + (k-2)^{\alpha+1}(2-2k-\alpha)\Big),\\
&k = 2,3,...,n,\\
&\sigma_1 = 3\alpha+4,\\
&\sigma_k = (k-2)^{\alpha+1}(2k+\alpha-2) - 2(k-2)^{\alpha}(2+\alpha)(1+\alpha) - (k)^{\alpha+1}(2k-6-3\alpha),\\
&k = 2,3,...,n.
\end{aligned} \tag{3.3}$$

Proof. First, for $\phi_i(t)$, $i = 0,...,n$, we have the definition of the Riemann-Liouville integral operator as follows

$$I_t^{\alpha}\phi_i(t) = \frac{1}{\Gamma(\alpha)}\int_0^t (t-\tau)^{\alpha-1}\phi_i(\tau)d\tau. \tag{3.4}$$

Now, we approximate the integral by an expression in terms of QHFs, as follows

$$I_t^{\alpha}\phi_i(t) \simeq \sum_{j=0}^{n}\gamma_{ij}\phi_j(t), \quad i = 0,...,n, \tag{3.5}$$

where the coefficients γ_{ij} are the values of $I_t^{\alpha}\phi_i(t)$, namely Eq. (3.4), at the jh point. Thus, we have

$$\gamma_{ij} = \frac{1}{\Gamma(\alpha)}\int_0^{jh} (jh-\tau)^{\alpha-1}\phi_i(\tau)d\tau, \quad i,j = 0,1,...,n. \tag{3.6}$$

Using Eqs. (2.5-2.6), we calculate the integral (3.6). For even i's, and even n, $i = 0,2,...,n$, by substituting (2.5) in (3.6), we introduce the coefficients as follows:

$$\gamma_{ij} = \begin{cases} 0, & j \le i,\\ \frac{h^{\alpha}}{2\Gamma(\alpha+3)}\left(\alpha(2\alpha+3)\right), & j = i+1,\\ \frac{h^{\alpha}}{2\Gamma(\alpha+3)}\left(\begin{array}{l}(j-i)^{\alpha+1}(2j-2i-3\alpha-6)\\ +2(j-i)^{\alpha}(\alpha+1)(\alpha+2)\\ -(j-i-2)^{\alpha+1}(2j-2i-2+\alpha)\end{array}\right), & j > i+1.\end{cases} \tag{3.7}$$

Now we attain (3.6) for odd i's:

$$\gamma_{ij} \simeq \begin{cases} 0, & j < i,\\ \frac{h^{\alpha}}{2\Gamma(\alpha+3)}(3\alpha+4), & j = i,\\ \frac{h^{\alpha}}{2\Gamma(\alpha+3)}\left(\begin{array}{l}(j-i-1)^{\alpha+1}(2j-2i+\alpha)\\ -2(j-i-1)^{\alpha}(\alpha+1)(\alpha+2)\\ -(j-i+1)^{\alpha+1}(2j-2i-3\alpha-4)\end{array}\right), & j > i.\end{cases} \tag{3.8}$$

Consider $2k^{'} = i$ in Eqs. (3.7), $2k^{'}+1 = i$ in Eqs. (3.8), then apply $2k^{'}+k = j$ to both Eqs. (3.7, 3.8), $k^{'}, k = 0,...,n$. Some simple manipulations completes the proof. □

For instance, when $\alpha = 1$, for the operational matrix (3.2), and even n, we get

$$\begin{aligned}
&\rho_1 = 5, \;\; \rho_k = 4, \;\; k = 2,...,n,\\
&\sigma_1 = 7, \;\; \sigma_k = 20, \;\; k = 2,...,n.
\end{aligned} \tag{3.9}$$

In order to approximate a non-linear function with QHFs, we can use (2.16) and (3.1), as follows:

$$I_t^{\alpha}u^m(t) \simeq I_t^{\alpha}\left(\sum_{i=0}^{n} a_i^m\phi_i(t)\right) \simeq I_t^{\alpha}\left(\mathrm{A}_m^T\Phi(t)\right) \simeq \mathrm{A}_m^T Q^{\alpha}\Phi(t), \quad m = 1,2,.... \tag{3.10}$$

4. Error Analysis

This section aims to determine a formula for the absolute error when we approximate a function with QHFs. Let us approximate a function $u(t)$, as (2.7). So we have

$$u_n(t) = \sum_{i=0}^{n} u(ih)\phi_i(t), \tag{4.1}$$

for $t \in (jh,\ (j+1)h)$, $j = 0,\ 2,\ 4, ..., n$, $h = T/n$, and even n, using $(2.5 - 2.6)$ and doing some computation, we obtain

$$\begin{aligned} u_n(t) &= \sum_{i=0}^{n} u(ih)\phi_i(t) = u(jh)\phi_j(t) + u(jh+h)\phi_{j+1}(t) \\ &= u(jh)\left(\frac{(t-(j+1)h)\left((t-(j+2)h)\right)}{2h^2}\right) + u(jh+h)\left(\frac{(t-(j)h)\left((t-(j+3)h)\right)}{-2h^2}\right) \\ &= u(jh)\left(\frac{\left((t-jh)^2 - 3h(t-jh) + 2h^2\right)}{2h^2}\right) - u(jh+h)\left(\frac{(t-jh)^2 - (t-jh)3h}{2h^2}\right) \\ &= u(jh) + (t-jh)\left(\frac{-3u(jh) + 3u(jh+h)}{2h}\right) - \frac{(t-jh)^2}{2h}\left(\frac{u(jh+h) - u(jh)}{h}\right), \end{aligned}$$

thus, assuming $h \to 0$, for even n and $j = 0,\ 2,\ 4, ..., n$, one has

$$u_n(t) = u(jh) + \frac{3}{2}(t-jh)u'(jh) - \frac{(t-jh)^2}{2h}u'(jh) + O(t-jh)^2. \tag{4.2}$$

A two terms Taylor expansion of $u(t)$ around the point $t = jh$ can be written as the following,

$$u(t) = \sum_{k=0}^{1} \frac{(t-jh)^k}{k!}u^{(k)}(jh) + O(t-jh)^2. \tag{4.3}$$

The difference operation of (4.2) from (4.3) yields to

$$u_n(t) - u(t) = \frac{1}{2}\left((t-jh) - \frac{(t-jh)^2}{h}\right)u'(jh) + O(t-jh)^2. \tag{4.4}$$

Let $E = \{k \in Q|\ \forall t, h,\ t = kh\}$, result in

$$u_n(kh) - u(kh) = \frac{hf'(jh)}{2}\left((k-j)(1-(k-j))\right) + O((k-j)h)^2, \tag{4.5}$$

where $k \in (j,\ j+1)$. Also, for $t \in (jh,\ (j+1)h)$, $j = 1,\ 3,\ 5, ..., n-1$, $h = T/n$, and even n, we get

$$\begin{aligned} u_n(t) &= \sum_{i=0}^{n} u(ih)\phi_i(t) = u(jh-h)\phi_{j-1}(t) + u(jh)\phi_j(t) \\ &= u(jh-h)\left(\frac{(t-jh)\left((t-(j+1)h)\right)}{2h^2}\right) + u(jh)\left(\frac{(t-(j-1)h)\left((t-(j+2)h)\right)}{-2h^2}\right) \\ &= u(ih) + \frac{(t-jh)}{2}\left(\frac{u(jh) - u(jh-h)}{h}\right) - \frac{(t-jh)^2}{2h}\left(\frac{u(jh) - u(jh-h)}{h}\right). \end{aligned}$$

So, assuming $h \to 0$, for even n and $j = 1,\ 3,\ 5, ..., n-1$, results in

$$u_n(t) = u(jh) + \frac{1}{2}(t-jh)u'(jh) - \frac{(t-jh)^2}{2h}u'(jh) + O(t-jh)^2. \tag{4.6}$$

From (4.6), for the absolute error at the points $t \in (jh,\, (j+1)h)$, we have

$$u(t) - u_n(t) = \frac{1}{2}\left((t-jh) + \frac{(t-jh)^2}{h}\right) u'(jh) + O(t-jh)^2, \tag{4.7}$$

Let $E = \{\forall t, h,\ \ \exists k \in Q,\ t = kh\}$, for $t \in (jh,\, (j+1)h)$, and even n, $j = 1, 3, ..., n-1$, $h \to 0$, one obtains

$$u(kh) - u_n(kh) = \frac{hu'(jh)}{2}\left((k-j)(1+k-j)\right) + O((k-j)h)^2. \tag{4.8}$$

where $k \in (j,\, j+1)$. Finally, for $t \in (jh,\, (j+1)h)$, $j = 0, 1, 2, ..., n$ and $h \to 0$ using (4.5) and (4.8), we have

$$|u(t) - u_n(t)| = \frac{h\,|u'(jh)|}{2}\left|(k-j)(1+(-1)^{j+1}(k-j))\right| + O\left(\frac{(k-j)}{h}\right)^2. \tag{4.9}$$

Since $k \in (j,\, j+1)$ and $nh = T$, from (4.9), we get

$$|u(t) - u_n(t)| \le \frac{T\,|u'(jh)|}{n} + O\left(\frac{1}{n^2}\right). \tag{4.10}$$

In the case of $k \to j$, $j = 0, ..., n$, we attain

$$|u(jh) - u_n(jh)|\ \to 0, \tag{4.11}$$

and $\forall k$, as $h \to 0$ or $n \to \infty$, we get

$$|u(t) - u_n(t)|\ \to 0. \tag{4.12}$$

5. Numerical algorithm

In this section, a numerical algorithm is offered to solve the problem (1.1). Consider the following fractional Duffing equation

$$\begin{aligned} &{}_0^C D_t^\beta u(t) + \mu_0\, {}_0^C D_t^\alpha u(t) = g(t) + \sum_{k=1}^{4} \mu_k \left(u^{2k-1}(t)\right),\ \ 1 < \beta \le 2,\ \ 0 < \alpha \le 1, \\ &u^{(i)}(0) = u_0^{(i)},\ \ i = 0, 1, ..., \lceil \beta \rceil - 1, \end{aligned} \tag{5.1}$$

First, by applying Riemann–Liouville integral operator of order β on the both sides of Eq. (5.1), one gets

$$I_t^\beta({}_\circ^C D_t^\beta u(t)) + \mu_0 I_t^\beta({}_\circ^C D_t^\alpha u(t)) = I_t^\beta g(t) + I_t^\beta\left(\sum_{k=1}^{4} \mu_k \left(u^{2k-1}(t)\right)\right). \tag{5.2}$$

Because of (2.3) and (2.4) we have

$$I_t^\beta({}_\circ^C D_t^\beta u(t)) = u(t) - u(0) - u'(0)t, \quad 1 < \beta \le 2, \tag{5.3}$$

$$I_t^\beta({}_\circ^C D_t^\alpha u(t)) = \left(I_t^{\beta-\alpha} u(t)\right) - \left(I_t^{\beta-\alpha} u(0)\right), \quad 0 < \alpha \le 1, \quad \alpha < \beta,$$

then, taking (2.2) into account:

$$I_t^\beta({}_\circ^C D_t^\alpha u(t)) = \left(I_t^{\beta-\alpha} u(t)\right) - \frac{u(0)}{\Gamma(\beta-\alpha+1)}\left(t^{\beta-\alpha}\right),\ 0 < \alpha \le 1,\ \ \alpha < \beta. \tag{5.4}$$

Substituting Eqs. (5.3)- (5.4) into Eq. (5.2), we get:

$$u(t) + \mu_0\left(I_t^{\beta-\alpha} u(t)\right) - \sum_{k=1}^{4} \mu_k I_t^\beta \left(u^{2k-1}(t)\right) - I_t^\beta g(t) - w(t) = 0, \tag{5.5}$$

where

$$w(t) = u(0) + u'(0)t + \frac{\mu_0 u(0)}{\Gamma(\beta-\alpha+1)}\left(t^{\beta-\alpha}\right).$$

Using (2.7) and (2.16), the functions $u^{2k-1}(t)$, $g(t)$ and $w(t)$ can be expressed in terms of QHFs as follows

$$u^{2k-1}(t) \simeq \sum_{i=0}^{n} {a_i}^{2k-1}\phi_i(t) = \mathrm{A}_{2k-1}^T\Phi(t), \quad \mathrm{A}_{2k-1} = [a_0^{2k-1}, a_1^{2k-1}, ..., a_n^{2k-1}]^T, \qquad k = 1, 2, 3, 4, \tag{5.6}$$

$$g(t) \simeq \sum_{i=0}^{n} g(ih)\psi_i(t) = G^T\Psi(t), \qquad G = [g(0), g(h), ..., g(nh)]^T, \tag{5.7}$$

and

$$w(t) \simeq \sum_{i=0}^{n} w(ih)\psi_i(t) = W^T\Psi(t), \qquad G = [W(0), W(h), ..., W(nh)]^T, \tag{5.8}$$

wherein n is an even positive integer. Utilizing (3.1), (3.2), and (3.10) and substitution of (5.6-5.8) in Eq. (5.5) results in,

$$A_1{}^T\Phi(t) + \mu_0\left(A_1Q^{(\beta-\alpha)}\Phi(t)\right) - \sum_{k=1}^{4}\mu_k A_{_{2k-1}}^T Q^{(\beta)}\Phi(t) - G^TQ^{(\beta)}\Phi(t) - W^T\Phi(t) = 0,$$

$$\left(A_1{}^T + \mu_0\left(A_1Q^{(\beta-\alpha)}\right) - \sum_{k=1}^{4}\mu_k A_{_{2k-1}}^T Q^{(\beta)} - G^TQ^{(\beta)} - W^T\right)\Phi(t) = 0,$$

$$A_1{}^T + \mu_0\left(A_1Q^{(\beta-\alpha)}\right) - \sum_{k=1}^{4}\mu_k A_{_{2k-1}}^T Q^{(\beta)} - G^TQ^{(\beta)} - W^T = 0, \quad 0 < \alpha \leq 1, \quad 1 < \beta \leq 2, \tag{5.9}$$

this system has the dimension $(n+1)\times(n+1)$. Suppose that

$$Q^{(\beta)} = [\gamma_{ij}], \qquad Q^{\beta-\alpha} = [\theta_{ij}], \qquad i, j = 0, 1, 2, ..., n, \tag{5.10}$$

so, from the operational matrix (3.2) one gets

$$\begin{aligned}
&\gamma_{i0} = \theta_{i0} = 0, && i = 0, 1, 2, ..., n, \\
&\gamma_{ni} = \theta_{ni} = 0, && i = 1, 2, ..., n, \\
&\gamma_{ij} = \theta_{ij} = 0, && j = 1, 3, ..., n-1, \qquad i = j+1, j+2, ..., n, \\
&\gamma_{ij} = \theta_{ij} = 0, && j = 2, 4, ..., n, \qquad i = j, j+1, ..., n.
\end{aligned}$$

Eq. (5.9) can be used to determine the unknown coefficients, starting to find the first unknown coefficient

$$a_0 = w(0), \tag{5.11}$$

in the next step, we have

$$eq_1: \quad a_1 + \mu_0\left[\sum_{i=0}^{1}\theta_{i1}a_i\right] - \left[\sum_{k=1}^{4}\sum_{i=0}^{1}\mu_k\gamma_{i1}a_i^{2k-1}\right] - \left[\sum_{i=0}^{1}g(ih)\gamma_{i1}\right] - w(h) = 0,$$

solving eq_1, a univariate equation, allows us to calculate a_1 and we can obtain a_2 as follows

$$eq_2: \quad a_2 = -\mu_0\left[\sum_{i=0}^{1}\theta_{i2}a_i\right] + \left[\sum_{k=1}^{4}\sum_{i=0}^{1}\mu_k\gamma_{i2}a_i^{2k-1}\right] + \left[\sum_{i=0}^{1}g(ih)\gamma_{i2}\right] + w(2h),$$

then

$$eq_3: \quad a_3 + \mu_0\left[\sum_{i=0}^{3}\theta_{i3}a_i\right] - \left[\sum_{k=1}^{4}\sum_{i=0}^{3}\mu_k\gamma_{i3}a_i^{2k-1}\right] - \left[\sum_{i=0}^{3}g(ih)\gamma_{i3}\right] - w(3h) = 0,$$

unknown parameter a_3 is calculated by solving eq_3, then we find a_4 as follows

$$eq_4: \quad a_4 = -\mu_0 \left[\sum_{i=0}^{3} \theta_{i4} a_i\right] + \left[\sum_{k=1}^{4}\sum_{i=0}^{3} \mu_k \gamma_{i4} a_i^{2k-1}\right] + \left[\sum_{i=0}^{3} g(ih)\gamma_{i4}\right] + w(4h),$$

The process can be continued up to the following.

$$eq_{n-1}: \quad a_{n-1} + \mu_0 \left[\sum_{i=0}^{n-1} \theta_{i(n-1)} a_i\right] - \left[\sum_{k=1}^{4}\sum_{i=0}^{n-1} \mu_k \gamma_{i(n-1)} a_i^{2k-1}\right] - \left[\sum_{i=0}^{n-1} g(ih)\gamma_{i(n-1)}\right] - w((n-1)h) = 0,$$

accordingly, after determining the value of the unknown coefficient a_{n-1} in this equation, the value of a_n will be determined as follows:

$$eq_n: \quad a_n = -\mu_0 \left[\sum_{i=0}^{n-1} \theta_{in} a_i\right] + \left[\sum_{k=1}^{4}\sum_{i=0}^{n-1} \mu_k \gamma_{in} a_i^{2k-1}\right] + \left[\sum_{i=0}^{n-1} g(ih)\gamma_{in}\right] + w(nh). \tag{5.12}$$

Therefore, by determining the coefficients, we can obtain an approximate solution via (2.7). To solve the nonlinear equations, see [32]. We utilized the MATLAB package to handle the computations. In order to illustrate the proposed method better, the following theorem is presented.

Theorem 5.1. *Consider the main problem Eq.(1.1). To obtain a numerical solution to Eq.(1.1) using QHFs, the following iterative algorithm in pseudocode is offered:*

Algorithm: *Quasi − hat functions for Duffing equations*

1 *Input* n *(even)*, $\alpha,\ \beta,\ \mu_k,\ k = 0, 1, ..., 4,\ T,\ g(t),\ u(0),\ u'(0).$

2 *Set* $h = T/n,\ t_i = ih,\ i = 0, ..., n.$

3 $w(t) = u(0) + u'(0)t + \dfrac{\mu_0 u(0)}{\Gamma(\beta-\alpha+1)}\left(t^{\beta-\alpha}\right).$

4 ▷ *Compute the elements of* $Q^{(\beta)} = [\theta_{ij}]$, *and* $Q^{(\beta-\alpha)} = [\gamma_{ij}],\ i, j = 0, ..., n.$

5 ▷ *Set and solve recursive univariate* ***equation v***, $v = 1, 3, 5, ...,\ n-1.$

$a_0 \leftarrow w(0)$

for $v = 1$ *to* $n-1$, $v =$ *odd number*

▷ *solution of the* v^{th} *equation* v, *determines the unknown parameter.*

$$equation\, v: \left\{ a_v + \mu_0 \left[\sum_{i=0}^{v} \theta_{iv} a_i\right] - \left[\sum_{k=1}^{4}\sum_{i=0}^{v} \mu_k \gamma_{iv} a_i^{k}\right] - \left[\sum_{i=0}^{v} g(ih)\gamma_{iv}\right] - w(vh) = 0\right.$$

▷ *and we can get*

$$a_{v+1} = -\mu_0 \left[\sum_{i=0}^{v} \theta_{i(v+1)} a_i\right] + \left[\sum_{k=1}^{4}\sum_{i=0}^{v} \mu_k \gamma_{i(v+1)} a_i^{k}\right] + \left[\sum_{i=0}^{v} g(ih)\gamma_{i(v+1)}\right] + w((v+1)h).$$

6 ▷ *Calculate fully* $a_i,\ i = 0, 1, ..., n.$

7 ▷ *Define QHFs* : $(\phi_i(t)),\ i = 0, 1, ..., n.$

8 ▷ *Determine the approximate solutions* : $u_n(t) = \sum_{i=0}^{n} a_i \phi_i(t).$

6. Convergence Analysis

In this section, we will verify the convergence of the numerical solution based on the proposed method.

Theorem 6.1. *Let* $u_n(t)$, $t \in (ih, (i+1)h)$, $i = 0,\ 1,\ 2,\ ..., n$, $h = T/n$, *and even* n, *be the numerical solution of Eq. (1.1) obtained by the method proposed in section 5,* $u(t)$ *is its exact solution and* $E_n(t)$ *is the residual error for the numerical solution. Also, suppose* d, $\overline{d}$, b, *and* M *are positive constants such that* $|u'(t)| \leq \mathrm{M}$. *Then,* $E_n(t)$ *tends to*

zero, when $n \to \infty$*, where*
$d = \sup_{t,\tau\in[0,T]} \left|\Gamma^{-1}(\beta-\alpha)(t-\tau)^{\beta-\alpha-1}\right|$, $\overline{d} = \sup_{t,\tau\in[0,T]} \left|L\Gamma^{-1}(\beta)(t-\tau)^{\beta-1}\right|$, *and* $b = \sup\left\{\frac{T}{n} + O\left(\frac{1}{n^2}\right)\right\}$.

Proof. Applying (2.3) and (5.5), it is suitable to rewrite Eq. (1.1) in the integral form

$$u(t) + \mu_0\left(I_t^{\beta-\alpha}u(t)\right) - \sum_{k=1}^{4}\mu_k I_t^{\beta}\left(u^{2k-1}(t)\right) - I_t^{\beta}g(t) - w(t) = 0, \tag{6.1}$$

wherein

$$w(t) = u(0) + u'(0)t + \frac{\mu_0 u(0)}{\Gamma(\beta-\alpha+1)}\left(t^{\beta-\alpha}\right),\ 0<\beta\le 2,\ 0<\alpha\le 1,\ t\in I(t),$$

thus, $u_n(t)$ satisfies the following equation

$$u_n(t) + \mu_0\left(I_t^{\beta-\alpha}u_n(t)\right) - \sum_{k=1}^{4}\mu_k I_t^{\beta}\left(u_n^{2k-1}(t)\right) - I_t^{\beta}g(t) - w(t) + E_n(t) = 0. \tag{6.2}$$

The residual function $E_n(t)$ can be obtained by using the following relation

$$E_n(t) = e_n[u](t) + J_n^{\beta-\alpha}[u](t) - V_n^{\beta}[u^{2k-1}](t), \tag{6.3}$$

where

$$e_n[u](t) = u(t) - u_n(t), \tag{6.4}$$

$$J_n^{\beta-\alpha}[u](t) = \frac{\mu_0}{\Gamma(\beta-\alpha)}\int_0^t (t-\tau)^{\beta-\alpha-1}(u(\tau)-u_n(\tau))d\tau, \tag{6.5}$$

and

$$V_n^{\beta}[u^{2k-1}](t) = \sum_{k=1}^{4}\frac{\mu_k}{\Gamma(\beta)}\int_0^t (t-\tau)^{\beta-1}(u^{2k-1}(\tau) - u_n^{2k-1}(\tau))d\tau. \tag{6.6}$$

Then, we attain

$$|E_n(t)| \le |e_n[u](t)| + \left|J_n^{\beta-\alpha}[u](t)\right| + \left|V_n^{\beta}[u^{2k-1}](t)\right|. \tag{6.7}$$

For $t\in(ih,\ (i+1)h)$, $i=0,\ 1,\ 2,...,n$, using (4.10), the approximation of the absolute error using QHFs yields

$$|u(t)-u_n(t)| \le \frac{T\,|u'(jh)|}{n} + O\left(\frac{1}{n^2}\right). \tag{6.8}$$

By using (6.8), we have

$$|e_n[u](t)| \le \frac{Mb}{n}, \tag{6.9}$$

where $|u'(ih)|\le M$ and $b = \sup\left\{\frac{T}{n}+O\left(\frac{1}{n^2}\right)\right\}$. As $n\to\infty$, $|e_n[u](t)|\to 0$. In addition, the following inequality holds [7]

$$\left|u^{2k-1}(t) - u_n^{2k-1}(t)\right| \le (2k-1)L\,|u(t)-u_n(t)|,\ k=1,2,3,4, \tag{6.10}$$

where $L = \left|(\max(u(t), u_n(t)))^{2k-2}\right|$. Then, by using (6.5) and (6.8), we get

$$\begin{aligned}\left|J_n^{\beta-\alpha}[u](t)\right| &= \frac{\mu_0}{\Gamma(\beta-\alpha)}\left|\int_0^t (t-\tau)^{\beta-\alpha-1}(u(\tau)-u_n(\tau))d\tau\right| \\ &\leq \frac{|\mu_0|}{\Gamma(\beta-\alpha)}\int_0^t (t-\tau)^{\beta-\alpha-1}\left|u(\tau)-u_n(\tau)\right|d\tau \\ &\leq \frac{M|\mu_0|}{2n}db, \end{aligned} \tag{6.11}$$

wherein $|u'(ih)| \leq M$, $d = \sup\limits_{t,\tau\in[0,T]}\left|\Gamma^{-1}(\beta-\alpha)(t-\tau)^{\beta-\alpha-1}\right|$, $b = \sup\left\{\frac{T}{n} + O\left(\frac{1}{n^2}\right)\right\}$. As $n \to \infty$, $\left|J_n^{\beta-\alpha}[u](t)\right| \to 0$. As well, from (6.6), (6.8) and (6.10), we have

$$\begin{aligned}\left|V_n^{\beta}[u^{2k-1}](t)\right| &= \sum_{k=1}^{4}\frac{1}{\Gamma(\beta)}\left|\mu_k\int_0^t (t-\tau)^{\beta-1}(u^{2k-1}(\tau)-u_n^{2k-1}(\tau))d\tau\right| \\ &\leq \sum_{k=1}^{4}\frac{|\mu_k|}{\Gamma(\beta)}\int_0^t (t-\tau)^{\beta-1}\left|(u^{2k-1}(\tau)-u_n^{2k-1}(\tau))\right|d\tau \\ &\leq \sum_{k=1}^{4}\frac{(2k-1)\left|\mu_k\right|M}{2n}\bar{d}b \leq \sum_{k=1}^{4}\frac{(2k-1)\left|\mu^*\right|M}{2n}\bar{d}b, \end{aligned} \tag{6.12}$$

wherein
$|u'(ih)| \leq M$, $\bar{d} = \sup\limits_{t,\tau\in[0,T]}\left|L\Gamma^{-1}(\beta)(t-\tau)^{\beta-1}\right|$, $b = \sup\left\{\frac{T}{n} + O\left(\frac{1}{n^2}\right)\right\}$, and $\mu^* = Max\{\mu_k\}_{k=1}^{n}$. Therefore, as $n \to \infty$, $\left|V_n^{\beta}[u^{2k-1}](t)\right| \to 0$. As a result, from relations (6.9), (6.11), (6.12), and (6.7), it is evident that the residual function $|E_n(t)|$ tends to zero, as $h \to 0$, or $n \to \infty$. □

7. Numerical examples

In this section, the theoretical results of the previous sections are used for solving non-linear full fractional Duffing equations, i.e. initial condition equation (1.1). To assess the accuracy of the scheme, let us define the absolute error (AE) as

$$AE(t) = \left|u(t) - u_n(t)\right|,\ t \in [0,T], \tag{7.1}$$

and the logarithm of the l_∞-norm error (LE) as

$$LE = ln\left(\|e_n\|_\infty\right), \quad \|e_n\|_\infty = \sup_{[t_i=ih]_{i=0}^{n}}\left\{|u(t_i) - u_n(t_i)|\right\}, \tag{7.2}$$

Using these definitions, the convergence order with respect to this norm will be introduced as follows,

$$Order = \log_2\left(\frac{\|e_n\|_\infty}{\|e_{2n}\|_\infty}\right), \tag{7.3}$$

where $u_n(t),\ n = T/h$ is the approximate solution defined in (5.6). In addition, for different values of $1 < \beta \leq 2$ and $0 < \alpha \leq 1$, the resulting solutions are compared in the integer and fractional order with each other.

Example 7.1. Consider the following non-linear full fractional Duffing equation [25] :

$$\begin{aligned}&{}_0^C D_t^{\beta} u(t) + \mu_0 {}_0^C D_t^{\alpha} u(t) = g(t) + \sum_{k=1}^{4}\mu_k\left(u^{2k-1}(t)\right), \quad t \in [0,12], \\ &u(0) = 0.5, \ \ u'(0) = -0.5, \ \ \mu_0 = -2, \ \ \mu_1 = -1, \ \ \mu_2 = -8, \ \ \mu_3 = \mu_4 = 0, \ \ g(t) = e^{(-3t)}.\end{aligned}$$

Table 1. Numerical results of Example 7.1 for $T = 12$.

Points t	Exact solutions	Approximate solutions, $h = 1/16$	Approximate solutions, $h = 1/32$	Absolute errors $AE(t), h = 1/16$	Absolute errors $AE(t), h = 1/32$
0.0	0.5000000	0.5000000	0.5000000	0.0000000	0.0000000
1.5	0.1115651	0.1104659	0.1111333	1.0992×10^{-3}	4.3174×10^{-4}
3.0	0.0248935	0.0252859	0.0251236	3.9237×10^{-4}	2.3004×10^{-4}
4.5	0.0055545	0.0059159	0.0057434	3.6142×10^{-4}	1.8894×10^{-4}
6.0	0.0012394	0.0014107	0.0013269	1.7136×10^{-4}	8.7504×10^{-5}
7.5	0.0002765	0.0003418	0.0003095	6.5292×10^{-5}	3.2972×10^{-5}
9.0	0.0000617	0.0000839	0.0000728	2.2202×10^{-5}	1.1119×10^{-5}
10.5	0.0000138	0.0000208	0.0000173	7.0378×10^{-6}	3.4964×10^{-6}
12.0	0.0000031	0.0000052	0.0000041	2.1276×10^{-6}	1.0478×10^{-6}

Table 2. Absolute errors in Example 7.1 with the present scheme and block-pulse functions wavelet scheme.

Points t	QHFs, Absolute errors $AE(t),\ T = 12,\ h = 1/64$	QHFs, Absolute errors $AE(t),\ T = 12,\ h = 1/128$	BPFs Absolute errors [25]
0000	0000	0000	2.9762×10^{-3}
1.008	7.7834×10^{-4}	1.8912×10^{-4}	1.0924×10^{-3}
2.016	1.6993×10^{-5}	8.5987×10^{-6}	3.9923×10^{-4}
3.012	9.2580×10^{-5}	1.4390×10^{-5}	1.4726×10^{-4}
4.008	9.8168×10^{-5}	5.9454×10^{-5}	5.4206×10^{-5}
5.004	7.1876×10^{-5}	3.5439×10^{-5}	1.9913×10^{-5}
6.000	4.4182×10^{-5}	2.2196×10^{-5}	7.3004×10^{-6}
7.008	2.2324×10^{-5}	1.1684×10^{-5}	2.6387×10^{-6}
8.004	1.1337×10^{-5}	5.6373×10^{-6}	9.6327×10^{-7}
9.000	5.5597×10^{-6}	2.7794×10^{-6}	3.5087×10^{-7}
10.008	2.5186×10^{-6}	1.2830×10^{-6}	1.2596×10^{-7}
11.004	1.1512×10^{-6}	5.7251×10^{-7}	4.5672×10^{-8}
11.988	5.3294×10^{-7}	2.5800×10^{-7}	1.6717×10^{-8}

For $\beta = 2$ and $\alpha = 1$, the exact solution is $u(t) = 0.5e^{(-t)}$. Approximate numerical results using different values of $(n = T/h)$ are shown in Tables 1-3 and Figures 2-4. Table 1 shows the approximate and exact solutions and the absolute errors to the problem at some points. The elapsed time is 5.451 seconds for $T = 12, h = 1/32$. One can compare the accuracy of the numerical results reported in [25] that uses the wavelet method of block pulse functions (BPFs), with the results of the proposed method presented in Table 2. In accordance with the numerical results, Table 3 demonstrates that the theoretical conclusions in section 6 are confirmed by the order of convergence. Figure 2 indicates the behavior of absolute errors for Example 7.1. Also, Figure 3 shows the logarithm of the l_∞-norm errors. As can be seen from the plot, as n increases, the error decreases. In addition, the comparison of the results obtained for different values of β and α with the exact solutions of the equation are plotted in Figure 4. The elapsed computing is 95.871 seconds with values of $T = 12, h = 1/16$.

Example 7.2. Consider the following non-linear full fractional Duffing equation [25]:

$$
\begin{aligned}
&{}_0^C D_t^\beta u(t) + {}_0^C D_t^\alpha u(t) = \sin^3(t) + \cos(t) - u(t) - u^3(t),\ \ t \in [0, 12],\\
&u(0) = 0,\ \ u'(0) = 1.
\end{aligned}
$$

Table 3. Order of convergence of Example 7.1

$T,\ h$	$T=12,\ h=1/16$	$T=12,\ h=1/32$	$T=12,\ h=1/64$	$T=12,\ h=1/128$
Order of convergence	1.1408	1.0778	1.0401	–

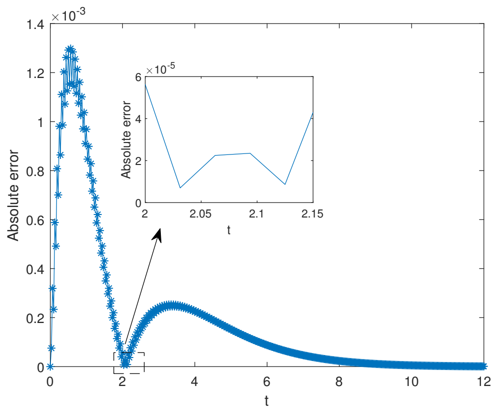

Figure 2. Absolute errors in Example 7.1 for $h = 1/32,\ T = 12$.

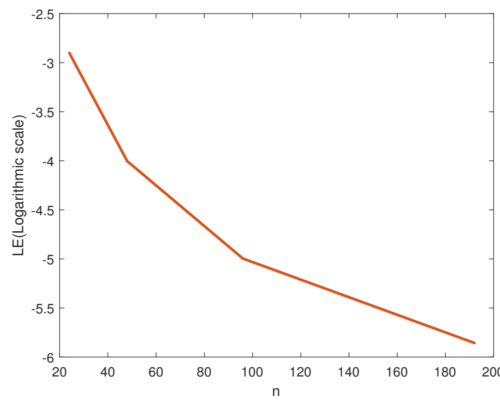

Figure 3. The logarithm of the $l_\infty-$norm error in Example 7.1.

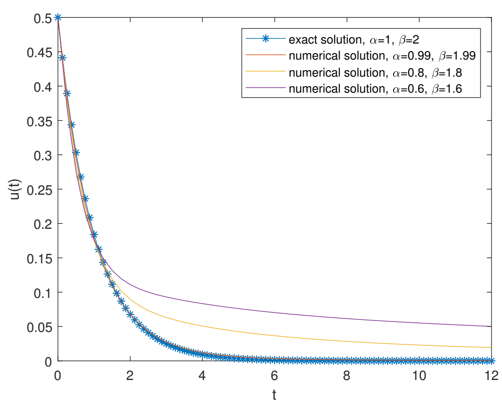

Figure 4. Exact and numerical solutions of Example 7.1 for h = 1/8, T = 12.

With the exact solution $u(t) = sin(t)$ for $\beta = 2$ and $\alpha = 1$. Approximate numerical results using different values of h are shown in Tables 4-5, and Figures 5-7. Table 4 indicates the approximate and exact solutions to the problem at some points. Numerically, the convergence order is 1.0147, as shown in Table 5. As displayed in Figure 5, the sinusoidal behavior of absolute errors in Example 7.2 is seen at $h = 1/32,\ T = 12$. Figure 6 shows that the logarithm of the l_∞-norm error decreases as n increases. Figure 7 can be used to compare the exact and approximate solutions of the Example 7.2 with different values of alpha and beta. The elapsed computing is 98.990 seconds with values of $T = 12, h = 1/16$.

TABLE 4. Numerical results of Example 7.2 for $T = 12$.

Points t	Exact solutions	Approximate solutions, $h = 1/16$	Approximate solutions, $h = 1/32$	Absolute errors $AE(t), h = 1/16$	Absolute errors $AE(t), h = 1/32$
0.0	0	0.0000000	0.0000000	0.0000000	0.0000000
1.5	0.9974950	1.0037069	1.0005409	6.2119×10^{-3}	3.0459×10^{-3}
3.0	0.1411200	0.1333742	0.1374687	7.7458×10^{-3}	3.6512×10^{-3}
4.5	-0.9775301	-0.9841707	-0.9807690	6.6406×10^{-3}	3.2389×10^{-3}
6.0	-0.2794155	-0.2719032	-0.2759009	7.5122×10^{-3}	3.5145×10^{-3}
7.5	0.9379999	0.9454781	0.9416436	7.4781×10^{-3}	3.6435×10^{-3}
9.0	0.4121185	0.4055898	0.4090723	6.5287×10^{-3}	3.0462×10^{-3}
10.5	-0.8796958	-0.8881699	-0.8838105	8.4742×10^{-3}	4.1146×10^{-3}
12.0	-0.5365729	-0.5307893	-0.5338842	5.7836×10^{-3}	2.6887×10^{-3}

TABLE 5. Order of convergence in Example 7.2.

$T,\ h$	$T = 12,\ h = 1/16$	$T = 12,\ h = 1/32$	$T = 12,\ h = 1/64$	$T = 12,\ h = 1/128$
Order of convergence	1.0552	1.0288	1.0147	–

Example 7.3. Consider the following strongly non-linear full fractional Duffing equation [25] :

$$
\begin{aligned}
&{}_0^C D_t^{\beta} u(t) +{}_0^C D_t^{\alpha} u(t) = g(t) - u(t) - u^3(t) - u^5(t)\ - u^7(t),\ t \in [0,1],\\
&u(0) = 0,\ \ u'(0) = 0,\ \ g(t) = t^{21}+t^{15}+t^9+t^3+3t^2+6t.
\end{aligned}
$$

For $\beta = 2$ and $\alpha = 1$, the exact solution is $u(t) = t^3$. Tables 6-7 and Figures 8-10 show approximate numerical results using different values of h. Table 6 shows the absolute errors in the problem at some grid points. Table 7 indicates the convergence order for various values of h. Figure 8 shows the behavior of absolute errors for the Example 7.3. Figure 9 shows the logarithm of the l_∞-norm errors. Also, a comparison of the results for different values of β and α with the exact solution of the equation are shown in Figure 10. The elapsed computing is 3.175 seconds with values of $T = 1, h = 1/16$.

Example 7.4. As a fourth example, consider the following non-linear full fractional Duffing equation [29]:

$$
\begin{aligned}
&{}_0^C D_t^2 u(t) + \mu_0 {}_0^C D_t^1 u(t) = g(t) + \sum_{k=1}^{4} \mu_k \left(u^{2k-1}(t)\right), \quad t \in [0,12],\\
&u(0) = 0.3,\ \ u'(0) = -2.3,\ \ \mu_0 = 0.4,\ \ \mu_1 = -1.1,\ \ \mu_2 = -1,\ \ \mu_3 = \mu_4 = 0,\ \ \ g(t) = 2.1\cos(1.8\ t).
\end{aligned}
$$

Due to the lack of an analytical solution, we compare the highest accuracy of approximate solutions using the hybrid Legendre polynomials and block-pulse functions wavelet method [29], the Laplace transform decomposition algorithms (LTDA) [33], and the Runge-Kutta method [29] with the proposed approaches. The obtained numerical results, shown in Table 8, are consistent with the numerical results presented in other articles. The hybrid Legendre polynomials and block-pulse functions wavelet method have two index values M and N, where $T/h = M \times N$. A comparison between changes in the integer and fractional orders of the equation is shown on Figure 11.

Example 7.5. Finally, we consider the following fractional oscillation equation [30]:

$$
\begin{aligned}
&{}_0^C D_t^{\beta} u(t) + \mu_0 {}_0^C D_t^{\alpha} u(t) = g(t) + \mu_1 u(t),\ t \in [0,1],\\
&u(0) = 0,\ \ u'(0) = 0,\ \ \mu_0 = 1,\ \ \mu_1 = -1,\ \ \ g(t) = 8.
\end{aligned}
$$

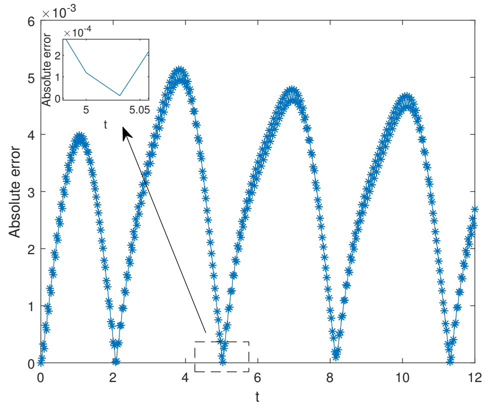

FIGURE 5. Absolute errors in Example 7.2 for h = 1/32, T = 12.

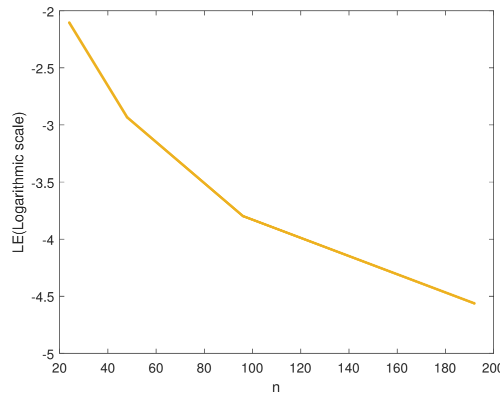

FIGURE 6. The logarithm of the $l_\infty-$norm error in Example 7.2.

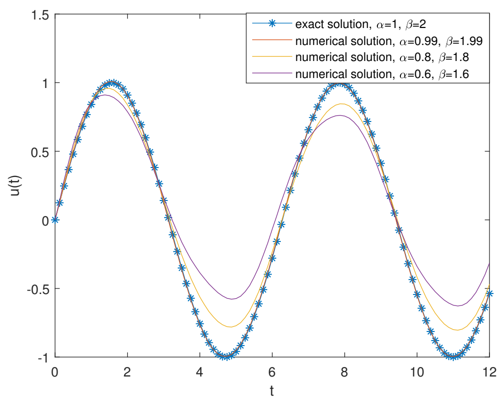

FIGURE 7. Exact and numerical solutions of Example 7.2 for h = 1/8, T = 12.

The problem has been solved by using hat functions (HFs) in [30], for $\beta = 2$, $\alpha = 0.5$, and $h = 0.001$. As shown in Table 9, we can compare our numerical results with those provided in [20, 22, 30]. By comparing the structure of operational matrices for HFs [30] and QHFs, it can be concluded that by using HFs, the main problem is reduced to solve n equations, while QHFs methods only need to solve $n/2$ equations; in the proposed algorithm, the even coefficients $a_i = u(ih)$, $i = 2, 4, ..., n$, are obtained by calculating the odd coefficients $a_i = u(ih)$, $i = 1, 3, ..., n-1$. The algorithm created from QHFs is a low-cost computational method. As can be seen, the proposed method obtained similar solutions to those obtained by other numerical methods. Table 10 displays the computing time (in seconds) to obtain the numerical solutions for Examples 7.1–7.5 with different values of h and $T = 1$.

8. Conclusion

QHFs have been used to solve the strongly nonlinear full fractional Duffing equations. Quasi-hat functions and the corresponding operational matrix are introduced. A one-step iterative numerical algorithm is created using the fractional-order operational matrix of integration and the proposed method to produce an approximate solution. An analysis of the method's absolute errors and convergence is conducted. Four numerical examples are provided to show

TABLE 6. Absolute errors at some selected points in Example 7.3 for $T = 1$.

Points t	Absolute errors $AE(t), h = 1/32$	Absolute errors $AE(t), h = 1/64$	Absolute errors $AE(t), h = 1/128$
0.000	0.0000000	0.0000000	0.0000000
0.125	1.1130×10^{-4}	8.6531×10^{-5}	5.0907×10^{-5}
0.250	6.5155×10^{-4}	3.8718×10^{-4}	2.0878×10^{-4}
0.375	1.5597×10^{-3}	8.7170×10^{-4}	4.5856×10^{-4}
5.000	2.7758×10^{-3}	1.5104×10^{-3}	7.8551×10^{-4}
0.625	4.2402×10^{-3}	2.2738×10^{-3}	1.1749×10^{-3}
0.750	5.8858×10^{-3}	3.1283×10^{-3}	1.6099×10^{-3}
0.875	7.5992×10^{-3}	4.0160×10^{-3}	2.0612×10^{-3}
1.000	8.9881×10^{-3}	4.7317×10^{-3}	2.4238×10^{-3}

TABLE 7. Order of convergence of Example 7.3.

$T,\ h$	$T = 1,\ h = 1/16$	$T = 1,\ h = 1/32$	$T = 1,\ h = 1/64$	$T = 1,\ h = 1/128$
Order of convergence	0.9018	0.9602	0.9828	–

TABLE 8. Numerical results of Example 7.4 with different methods.

Points t	QHFs, Approximate solutions, $h = 1/64$	QHFs, Approximate solutions, $h = 1/128$	LTDA [33]	Runge-Kutta [29]	Hybrid Legendre $M = 4,\ N = 16$, [29]
0.1	0.079653	0.082214	0.080942	0.083584	0.083592
0.2	−0.107693	−0.098764	−0.106822	−0.105092	−0.105084
0.3	−0.263951	−0.267737	−0.266147	−0.266020	−0.266012
0.4	−0.391726	−0.399292	−0.399536	−0.399978	−0.399970
0.5	−0.509322	−0.508825	−0.508129	−0.508315	−0.508308
0.6	−0.595238	−0.593869	−0.593180	−0.592891	−0.592885
0.7	−0.657697	−0.654563	−0.655381	−0.656066	−0.656062
0.8	−0.700860	−0.701437	−0.700417	−0.700677	−0.700675
0.9	−0.728874	−0.730068	−0.732272	−0.729971	−0.729971

TABLE 9. Numerical results of Example 7.5 with different methods for $\beta = 2$, $\alpha = 0.5$.

Points t	QHFs, Approximate solutions, $h = 1/1000$	HFs, Approximate solutions, $h = 1/1000$, [30]	BPF [20]	ADM $K = 50$, [22]
0.1	0.039751	0.039750	0.039754	0.039750
0.2	0.157044	0.157040	0.157043	0.157040
0.3	0.347394	0.347370	0.347373	0.347370
0.4	0.604745	0.604690	0.604699	0.604700
0.5	0.921854	0.921770	0.921768	0.921770
0.6	1.290591	1.290500	1.290458	1.290500
0.7	1.702201	1.702000	1.702007	1.702000
0.8	2.147549	2.147300	2.147286	2.147300
0.9	2.622130	2.617000	2.616998	2.617000
1.0	3.102327	3.101900	3.101902	3.101900

HFs: Hat functions, BPF: Block-pulse functions, ADM: Adomian decomposition method.

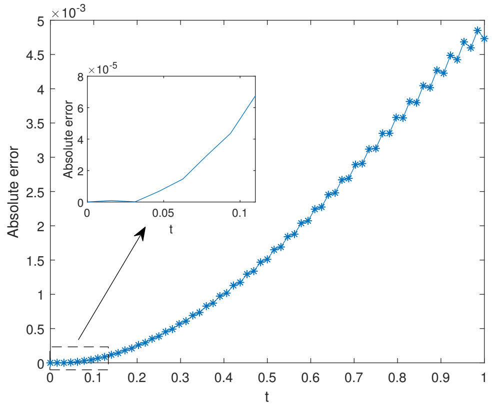

FIGURE 8. Absolute errors in Example 7.3 for h = 1/64.

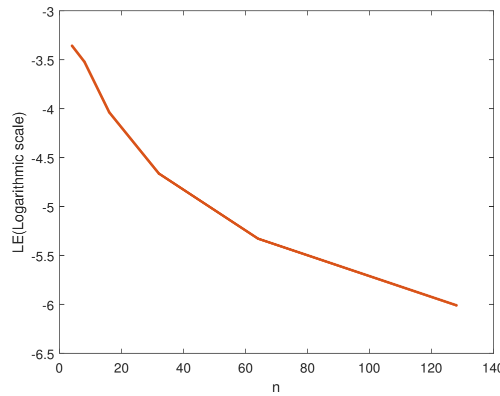

FIGURE 9. The logarithm of the $l_\infty -$ norm error in Example 7.3.

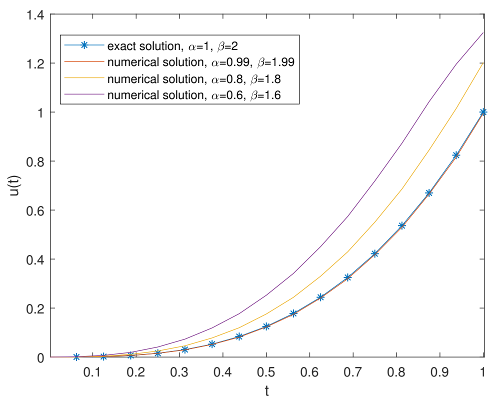

FIGURE 10. Exact and numerical solutions of Example 7.3 for h = 1/16.

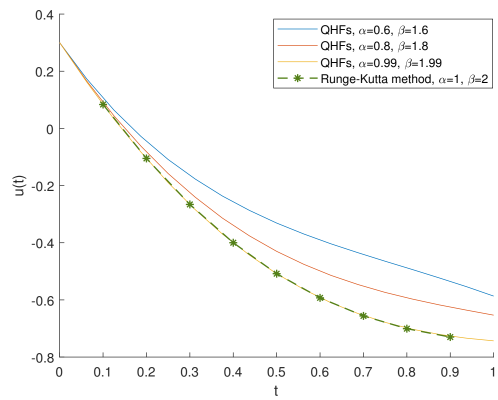

FIGURE 11. *Exact and numerical solutions of Example 7.4 for $h = 1/16$.*

the effectiveness of the new method. In Example 7.1, the absolute error is lower at the nodal points near the end of the interval, as shown in Figure 2. Table 2 shows the new method offers a more accurate solution at the beginning of the interval than the BPFs approaches. The numerical results in Example 7.2 confirm the sinusoidal behavior of the exact solution for this equation. In Example 7.3, the error clearly increases, as the time variable approaches one Figure 8.

In Examples 7.4 and 7.5, observing the numerical agreement of the proposed algorithm with some other numerical results proves its efficiency. A study of the results shows that, generally, as n increases, the accuracy of the approximate solution increases, and the absolute error decreases. One of the advantages of this proposed algorithm is that instead of solving a system of $(N+1)\times(N+1)$ equations, it needs only to solve $N/2$ univariate nonlinear equations. Finally, the proposed method (QHFs) can be used for a large number of similar problems such as the Bratu's equation and we will continue to work on developing this method.

Acknowledgements

We thank the anonymous reviewers for their careful reading of our manuscript and for giving constructive comments that can significantly help to improve the quality of the article.

TABLE 10. Complexity of Examples 7.1-7.5, for different values of h.

Length	$h = 1/16$	$h = 1/32$	$h = 1/64$	$h = 1/128$	$h = 1/256$
Example 7.1	1.419	3.873	11.628	40.262	147.069
Example 7.2	2.307	5.192	13.663	42.176	150.732
Example 7.3	3.175	9.216	30.586	118.940	442.113
Example 7.4	1.494	3.965	11.711	40.719	149.385
Example 7.5	1.358	3.725	10.217	32.189	113.027

REFERENCES

[1] B. N. Achar, J. W. Hanneken, and T. Clarke, *Response characteristics of a fractional oscillator*, Phys. A: Stat. Mech. Appl., *309*(3-4) (2002), 275–288.

[2] M. Ahmadi Darani and M. Nasiri, *A fractional type of the Chebyshev polynomials for approximation of solution of linear fractional differential equations*, Comput. Methods Differ. Equ., *1*(2) (2013), 96–107.

[3] H. A. Alyousef, A. H. Salas, M. R. Alharthi, and S. A. El-Tantawy, *Galerkin method, ansatz method, and He's frequency formulation for modeling the forced damped parametric driven pendulum oscillators*, J. Low Freq. Noise Vib. Act. Control., (2022), 14613484221101235

[4] I. Y. Aref'eva, E. Piskovskiy, and I. Volovich, *Oscillations and rolling for duffing's equation* , Quantum Bio-Informatics V, World Scientific, (2013), 37–48.

[5] P. Baratella and A. P. Orsi, *A new approach to the numerical solution of weakly singular volterra integral equations*, J. Comput. Appl. Math., *163*(2) (2004), 401–418.

[6] J. Biazar and H. Ebrahimi, *Orthonormal bernstein polynomials for volterra integral equations of the second kind*, Int. J. Appl. Math. Res., *9*(1) (2019), 9–20.

[7] J. Biazar and H. Ebrahimi, *A numerical algorithm for a class of non-linear fractional volterra integral equations via modified hat functions*, J. Integral Equ. Appl., *34*(3) (2022), 295–316.

[8] J. Biazar and R. Montazeri, *Optimal homotopy asymptotic and multistage optimal homotopy asymptotic methods for solving system of volterra integral equations of the second kind*, J. Appl. Math., 2019 (2019).

[9] T. Chen, X. Cao, and D. Niu, *Model modification and feature study of duffing oscillator* , J. Low Freq. Noise Vib. Act. Control., *41*(1) (2022), 230–243.

[10] M. Erfanian and A. Mansoori, *Solving the nonlinear integro-differential equation in complex plane with rationalized haar wavelet*, Math. Comput. Simul., *165* (2019), 223–237.

[11] X. Han and X. Guo, *Cubic hermite interpolation with minimal derivative oscillation*, J. Comput. Appl. Math., *331* (2018), 82–87.

[12] B. Hasani Lichae, J. Biazar, and Z. Ayati, *Asymptotic decomposition method for fractional order Riccati differential equation*, Comput. Methods Differ. Equ., *9*(1) (2022), 63–78.

[13] J. H. He and Y. O. El-Dib, *The reducing rank method to solve third-order duffing equation with the homotopy perturbation*, Numer. Methods Partial Differ. Equ., *37*(2) (2021), 1800–1808.

[14] J. H. He, *Taylor series solution for a third order boundary value problem arising in architectural engineering*, Ain Shams Eng. J., *11*(4) (2020), 1411–1414.
[15] S. Heydary and A. Aminataei, Numerical solution of Drinfel'd–Sokolov system with the Haar wavelets method, Comput. Methods Differ. Equ., (2022).
[16] K. Issa, B. M. Yisa, and J. Biazar, *Numerical solution of space fractional diffusion equation using shifted Gegenbauer polynomials*, Comput. Methods Differ. Equ., *10*(2) (2022), 431–444.
[17] I. Kovacic and M. J. Brennan, The Duffing equation: nonlinear oscillators and their behaviour, John Wiley & Sons, 2011.
[18] S. Lal and P. Kumari, *Approximation of functions with bounded derivative and solution of riccati differential equations by jacobi wavelet operational matrix*, Appl. Math. Comput., *394* (2021), 125834.
[19] C. Li and W. Deng, *Chaos synchronization of fractional-order differential systems*, Int. J. Mod. Phys. B., *20*(07) (2006), 791–803.
[20] Y. Li and N. Sun, *Numerical solution of fractional differential equations using the generalized block pulse operational matrix*, Comput. Math. Appl., *62*(63) (2011), 1046-1054.
[21] S. Mockary, A. Vahidi, and E. Babolian, *An efficient approximate solution of Riesz fractional advection-diffusion equation*, Comput. Methods Differ. Equ., *10*(2) (2022), 307–319.
[22] S. Momani and Z. Odibat, *Numerical comparison of methods for solving linear differential equations of fractional order*, Chaos, Solitons & Fractals, *31* (2007), 1248-1255.
[23] E. Montagu and J. Norbury, *Bifurcation tearing in a forced duffing equation*, J. Differ. Equ., *300* (2021), 1–32.
[24] S. Nourazar and A. Mirzabeigy, *Approximate solution for nonlinear duffing oscillator with damping effect using the modified differential transform method*, Sci. Iran. *20*(2) (2013), 364–368.
[25] P. Pirmohabbati, A. R. Sheikhani, H. S. Najafi, and A. A. Ziabari, *Numerical solution of full fractional duffing equations with cubic-quintic-heptic nonlinearities*, AIMS Math, *5*(2) (2020), 1621–1641.
[26] I. Podlubny, *Fractional differential equations*, Mathematics in Science and Engineering, Academic Press New York, 1999.
[27] J. Rad, S. Kazem, and K. Parand, *A numerical solution of the nonlinear controlled duffing oscillator by radial basis functions*, Comput. Math. with Appl. *64*(6) (2012), 2049–2065.
[28] M. Rasty and M. Hadizadeh, *A product integration approach based on new orthogonal polynomials for nonlinear weakly singular integral equations*, Acta Appl. Math., *109*(3) (2010), 861–873.
[29] L. Torkzadeh, *Numerical behavior of nonlinear duffing equations with fractional damping*, Rom. Rep. Phys., *73* (2021), 113.
[30] M. P. Tripathi, V. K. Baranwal, R. K. Pandey, and O. P. Singh, *A new numerical algorithm to solve fractional differential equations based on operational matrix of generalized hat functions*, Commun. Nonlinear Sci. Numer. Simul., *18*(6) (2013), 1327-1340.
[31] J. Wang, J. Zhou, and B. Peng, *Weak signal detection method based on duffing oscillator*, Kybernetes, *38*(10) (2009), 1662–1668.
[32] Z. Yang, *Gröbner bases for solving multivariate polynomial equations*, Computing Equilibria and Fixed Points, Springer, 1999, 265–288.
[33] E. Yusufoğlu, *Numerical solution of duffing equation by the laplace decomposition algorithm*, Appl. Math. Comput., *177*(2) (2006), 572–580.
[34] H. Zhang, Y. Mo, and Z. Wang, *A high order difference method for fractional sub- diffusion equations with the spatially variable coefficients under periodic boundary conditions*, J. Appl. Anal. Comput., *10*(2) (2020), 474–485.